



Research report

Functional brain networks during picture encoding and recognition in different odor contexts



J.L. Reichert^{a,b}, M. Ninaus^c, W. Schuehly^d, C. Hirschmann^a, D. Bagga^{a,b}, V. Schöpf^{a,b,*}

^a Institute of Psychology, University of Graz, Graz, Austria

^b BioTechMed Graz, Graz, Austria

^c Leibniz-Institut für Wissensmedien, Tübingen, Germany

^d Institute of Zoology, University of Graz, Graz, Austria

ARTICLE INFO

Keywords:

Olfaction

fMRI

Context-dependent memory

Episodic memory

Picture memory

Functional connectivity

ABSTRACT

Contextual odors can serve as retrieval cues when applied during encoding and recall/recognition of information. To investigate the neuronal basis of these observations, we collected functional MRI data while participants ($n = 51$) performed an encoding and recognition memory task during which odors (congruent: CO or incongruent: IO) were presented as contextual cues. Recognition performance was not influenced by odor, but there was increased activation in the piriform cortex during successful encoding in the CO group, possibly indicating enhanced retrieval of information previously integrated with an olfactory percept. Moreover, group-independent component analysis revealed a stronger task-modulation of subcortical networks for IO versus CO during the recognition task, pointing to differences in olfactory processing. These observations provide a deeper understanding of the involvement of functional neuronal networks in memory tasks and a basis for further evaluation of the impact of odor contexts.

1. Introduction

Our sense of smell is closely connected to episodic memory, as indicated by several studies showing that odors can evoke the recall of strong and emotional memories, often termed the ‘Proust effect’ [1–3]. When information is encoded in memory, the environmental context is encoded at the same time and can later serve as a cue facilitating memory retrieval. Indeed, a broad range of behavioral studies have found that odors can benefit memory performance when applied as congruent cues during encoding and recall/recognition tasks [4–11].

This peculiarity of the olfactory sense is related to the close anatomical connection between the primary olfactory cortex and limbic areas, such as the amygdala and the hippocampus, which play a key role in memory and emotional processing [12,13]. In contrast to other sensory modalities, olfactory signals are not relayed via the thalamus, but are transmitted to these areas by direct neural connections. Less is known, however, about the neuronal substrates of odor context-related effects. Previous studies indicate that the hippocampus plays an essential role in the encoding and retrieval of contextual information in general [14]. Odor context cues might lead to an enhanced recruitment of integrational networks comprising olfactory (e.g. piriform cortex, orbitofrontal cortex, entorhinal cortex, thalamus) and memory-related

regions (e.g. prefrontal cortex, medial-temporal regions) during successful encoding of information. Reinstatement of the odor context during memory retrieval might then facilitate memory performance and lead to a reactivation of these integrational networks during successful retrieval.

Functional neuronal networks have been extensively investigated during working memory tasks [15–19], but are relatively unexplored during episodic memory tasks [20,21]. In addition to traditional general linear model (GLM) analysis, in the current study we applied group independent component analysis (ICA) to encoding and recognition data in order to investigate the task-modulation of functionally connected brain networks. ICA has been shown to provide additional insights into investigation of functional networks, as this method is not constrained by experimental models and a priori information regarding expected temporal response patterns is not required [15,22,23]. In chemosensory stimulation paradigms in particular, a growing number of studies suggest that ICA can reveal supplemental information on processing pathways, compared with model-dependent analysis [24,25], possibly because of the complex dynamics of olfactory networks [25].

In the present study, participants performed an incidental encoding task, a free recall task and a yes/no recognition task while odors were

* Corresponding author at: Institute of Psychology University of Graz, Universitätsplatz 2, 8010 Graz, Austria.

E-mail addresses: Christina.hirschmann@gmx.at (C. Hirschmann), veronika.schoepf@uni-graz.at (V. Schöpf).

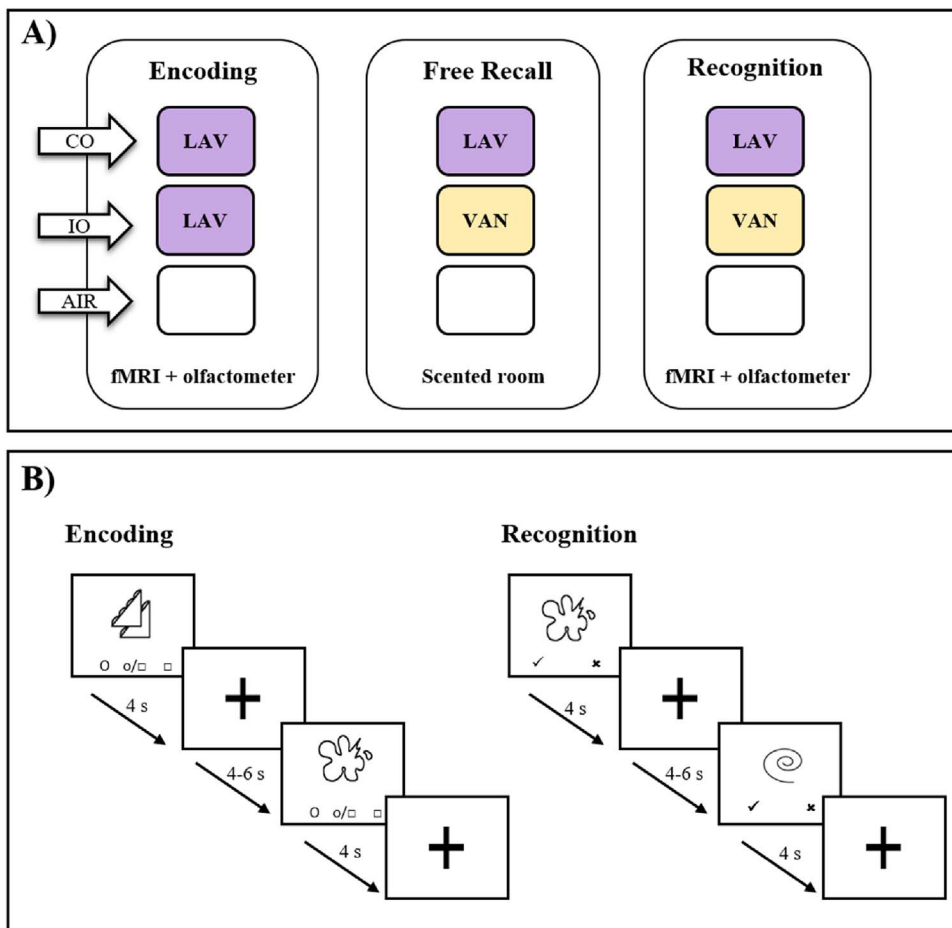


Fig. 1. (A) Summary of study procedure: odor presentation by study group. (B) Stimulus timing during the encoding and recognition task. LAV = lavender, VAN = vanilla. CO = congruent odor group, IO = incongruent odor group, AIR = control group receiving odorless air. Inter-stimulus-intervals were jittered as shown (duration 4–6 s). During the encoding task, participants evaluated whether the figure appeared predominantly round (index finger), had edges (ring finger) or was mixed (middle finger button press). During the recognition task, participants evaluated by button press whether or not they had previously seen the figure in the encoding task (yes = index finger, no = ring finger).

presented as contextual cues. Encoding and recognition tasks took place during functional magnetic resonance imaging (fMRI) (Fig. 1). Participants were randomly allocated to a congruent odor group (CO), an incongruent odor group (IO) or a control group (AIR, see Fig. 1). During the incidental encoding task, participants were shown abstract line drawings, while lavender odor was presented via an olfactometer (CO and IO groups only). During the subsequent free recall and recognition tasks, lavender odor was presented again for CO, while vanilla odor was presented for IO. We hypothesized that the congruent odor would enhance picture recognition performance and concurrently modify the memory-related activation of networks associated with context-dependent memory and those responsible for both olfactory and memory processing.

2. Experimental procedures

2.1. Subjects

A sample of 59 right-handed volunteers with normal olfactory function (assessed as described below) was recruited for the present study by means of public bulletins, e-mail lists and newspaper advertisements. The following exclusion criteria were applied: contraindications for MRI measurements (especially metallic implants, pacemakers, claustrophobia); cardiovascular, lung, chronic respiratory, neurological or psychiatric disease, diseases of the central nervous system and diseases affecting brain metabolism. Eight participants were excluded ($N = 5$ due to technical difficulties, $N = 1$ due to excessive movement during MRI measurements; $N = 2$ due to metallic implants). The remaining 51 participants were randomly allocated to a congruent odor group (CO), an incongruent odor group (IO) or a control group receiving only odorless air (AIR, see Table S1 for further sample

details). All participants were instructed to refrain from eating and drinking anything other than water one hour prior to testing, and from use of any scented products on the study day.

The study was approved by the local ethics committee and all participants provided written informed consent before participation. Participants were rewarded by course credits and by participation in a raffle for a coffee machine.

2.2. Procedure

2.2.1. Pre-study

Before the start of the fMRI study, a pre-study in 20 healthy normosmic participants (*mean* (*SD*) age = 26.31 (5.52), threshold discrimination identification (TDI, [26]) score = 36.86 (3.31), 10 female) was carried out to select the two odors used as contextual cues for the memory tasks. In this pre-study, a battery of 20 odors was scored for intensity, pleasantness, familiarity, and nameability. On the basis of these data, the two odors rated as most similar were chosen: vanilla [Alor vanilla oil; *mean* (*SD*) intensity = 7.15 (1.35), pleasantness = 6.65 (1.57), familiarity = 7.35 (1.84), nameability = 4.75 (3.01)] and lavender [Roth, CAS No. 90063-37-9; *mean* (*SD*) intensity = 7.55 (1.15), pleasantness = 6.80 (2.02), familiarity = 7.55 (1.85), nameability = 4.1 (3.34)].

2.2.2. Assessment of olfactory function

To qualify for inclusion in the fMRI study, all participants were pre-screened for normal olfactory function. Olfactory function was assessed with a standardized clinically approved test battery consisting of commercially available odorant pens ('Sniffin Sticks', Burghart Instruments, Wedel, Germany). The Sniffin' Sticks include a threshold test, a discrimination test, and an identification test to assess multiple

components of olfactory function (for a detailed description of the procedure see Hummel et al. [26]). During the threshold detection task, in each trial three pens were presented, with two pens (distractors) containing only the solvent and the third the target odorant (*n*-butanol) in different concentrations. Subjects were required to identify the odor-containing pen in a single-staircase forced-choice procedure. In the odor discrimination task, 16 triplets of pens were presented, with two containing the same, and one containing a different odorant. Subjects were required to determine which of three pens smelled differently from the other two. During the identification task, in a multiple-choice procedure, identification of individual odors was performed from lists of four descriptors provided for each odor. Scores range from 0 to 16 for the threshold, and from 1 to 16 for the discrimination and identification tasks. The subscores of the three tests were summed to determine the total threshold discrimination identification (TDI) score (see Table S1). Based on normative values [27], a normal olfactory function was defined by a TDI score > 30.3. The duration of the standardized olfactory testing was approximately 45 min.

2.2.3. Odor ratings

Before the start of the fMRI picture encoding task, an initial odor rating of five odors was carried out to familiarize all participants with the lavender and vanilla odors that were used in the later stages of the study. This initial rating was conducted to avoid that the novelty of the incongruent odor per se might influence the participants of the IO group, by e.g. increasing arousal during the recognition task. Participants were presented with five odors (ginger oil, vigoflor, vanilla, lemon, lavender) and asked to rate their intensity, familiarity, pleasantness and invigorating quality. For this rating, odors were dissolved in 1,2-propylene glycol in the following concentrations: 25% v/v for ginger oil, lavender, vanilla, and lemon oil and 50% v/v for vigoflor. Odors were presented in brown glass bottles filled with 1 mL of the respective odorant (soaked in cotton pads) and labeled with two-digit numbers.

2.2.4. Memory tasks

An overview of the memory tasks is provided in Fig. 1A. After the initial odor ratings, an incidental memory encoding task was carried out during fMRI scanning. In this task, participants were shown 60 abstract line drawings, while the lavender odorant was presented to the CO and IO groups via an olfactometer (see below) and odorless air to the AIR group. The line drawings used in the encoding and recognition tasks were selected from a set of nonsensical pictures [28]. Participants evaluated by button press whether the figure appeared predominantly round, had edges or was mixed. Before the encoding and recognition tasks, an instruction screen and 3–5 training trials were performed outside of the scanner to practice response button assignment. As a cover story for the incidental encoding task, participants were informed that the study investigated the influence of odors on the perception of shapes. For details see Fig. 1B. All button presses were recorded and carried out with the dominant right hand. Before and after the encoding task, 5-min resting-state MRI measurements were conducted. As these were unrelated to the present research focus, they are not considered further in the current study.

After a retention interval of approximately 40 min (*mean* = 42 min, *SD* = 7 min 40 s), a surprise free recall task was conducted in a scented room. During the retention interval, questionnaires regarding the individual significance of the sense of smell, mood (as assessed with a visual analogue scale, VAS, range 0–100, with 0 = not good at all, 100 = exceptionally good mood) and affective state (as assessed with the Positive and Negative Affect Schedule, PANAS [29], German version [30]), health status and cognitive processing strategies were conducted and sociodemographic data collected. For the free recall task, participants were asked to draw as many figures as they were able to remember from the encoding task on a sheet of paper during a 5-min period. The room was scented with lavender/vanilla, or not scented,

according to group allocation. The scent was created by adding 0.3 mL of the respective odorant (dissolved in 1,2-propylene glycol in the concentrations 1.75% v/v for lavender or 2.5% v/v for vanilla) to an odor diffusor (Aroflora 970 Stonelia). Odor concentrations were selected based on pretesting, to achieve a subtle odor impression that would not be noticed immediately by participants. To standardize the odor intensity, for each participant the diffusor was prepared approximately 25 min before the recall task started. After the free recall task, room ventilation was switched on to assure that the scents did not accumulate over time.

Subsequently, a yes/no recognition task was conducted in the MRI scanner. The order of stimulus presentation (the 60 previously shown figures from the encoding task and 60 new figures) was randomized for all participants. During the task, lavender was presented again for the CO group, while a vanilla odor was presented for IO and odorless air for AIR. Participants had to indicate by button press for each presented figure whether they had seen it previously or not. The computer-based tasks were operated by the software Presentation (Version 18.0, Neurobehavioral Systems, Inc., Berkeley, CA, www.neurobs.com).

During the MRI-based tasks, odors were presented using an MRI-compatible olfactometer described in detail by Lundström et al. [31]. In brief, the airflow through the olfactometer is controlled by solenoid valves, directing the odors through the odor glass reservoir (for CO/IO) or an empty glass reservoir (for AIR). The air used to operate the olfactometer was filtered using active carbon to avoid contamination by residual odors. The concentrations of vanilla (25% v/v in 1,2 propylene glycol) and lavender (5% v/v in 1,2 propylene glycol) were based on initial pretesting, with the aim of achieving a matched perceived odor intensity. A continuous odorless airstream of 1 L/min was transported to the birhinal nosepiece, masking tactile cues that might otherwise result from channel opening. At random intervals ranging from 5 to 12 s, the respective odor valve was opened for 500 ms, adding an additional odorized flow (0.5 L/min) to the continuous airstream. These settings were established after extensive pretesting, with the aim of achieving a continuous odor percept while at the same time avoiding adaptation effects. For AIR, an additional odorless flow (also 0.5 L/min) was added at the time points of stimulus presentation. After each of the two tasks, participants were interviewed outside of the scanner and rated the odor perceived during the task regarding different factors (intensity, pleasantness, familiarity, nameability and invigorating quality).

2.2.5. MRI image acquisition

fMRI data acquisition was carried out at a 3-T MRI (Siemens Skyra) using a 32-channel head coil. Fifty-two axial slices were acquired using a multiband EPI sequence (TR = 1.25 s, TE = 40 ms, FoV = 240 × 240 mm², Matrix size = 96 × 96, voxel size = 2.5 × 2.5 × 2.5 mm³). T1-weighted 3D gradient echo sequence scans (MPRAGE, 176 sagittal slices, TR = 1.56 s, TE = 2.07 ms, slice thickness = 1 mm, FoV = 256 × 256 mm²) were acquired coplanar with the functional scans for anatomical reference. Due to technical difficulties during data transmission, the last volumes of the recognition paradigm were lost for approximately 33% of the participants. Thus, in order to analyze the same quantity of data for every participant, the first 658 volumes of the recognition phase (approx. 90 of 120 trials) were analyzed for every participant.

2.2.6. Data analysis

2.2.6.1. Behavioral data analysis. Recalled figures were evaluated independently by three different raters. For each figure drawn by each participant, the raters determined whether it matched one of the 60 figures presented during encoding. Overall inter-rater reliability for the number of correctly recalled figures was ICC = 0.967 (ICC = intra-class correlation calculated as described in Hallgren [32]), indicating very good inter-rater agreement. Absolute numbers of correctly recalled figures were compared across groups via ANOVA (factor group)

followed by independent *t*-tests. For the picture recognition task, behavioral task performance (hit rates, false alarm rates, β and reaction times) for the three groups were compared using ANOVA (factor group) followed by independent *t*-tests. Hit rates, false alarm rates, d' and β were calculated according to signal detection theory [33]. As our study included both a recall task and a recognition task, memory or learning processes might have taken place during the recall task and might have impacted the subsequent recognition performance. Therefore, we additionally analyzed the recognition performance after removing the recalled items for each participant from the recognition data. Moreover, at three time points, mood (assessed by VAS = visual analogue scale) and affective state (as measured using the Positive and Negative Affect Schedule [29], German version [30]) of participants were assessed as control variables. Changes in these variables were assessed by mixed-measures ANOVA analyses (factors time point: pre/mid/post and group: CO/IO/AIR). The Statistical Package for the Social Sciences, Version 20.0 (SPSS, Chicago, Illinois) was used for data analysis.

2.2.6.2. Preprocessing of fMRI data. Data were preprocessed using SPM12 implemented in MatlabR2014b, including fieldmap distortion correction, motion correction, slice-time correction, spatial normalization using the DARTEL algorithm [34], and spatial smoothing (8-mm Gaussian kernel).

2.2.6.3. General linear model (GLM) analysis. Functional imaging data were analyzed using a two-level random-effects analysis. For individual-level analysis of the encoding task, the conditions “subsequent hits” and “subsequent misses” were modeled as regressors of interest, while for the recognition task, the conditions “hits”, “false alarms” “correct rejections” and “misses” were modeled. Thus, importantly, following previous fMRI episodic memory studies (e.g. [35–38]) the classification of trials for the encoding task was based on subsequent performance in the retrieval tasks (free recall/recognition tasks). For both tasks, six realignment parameters were included as regressors of no interest. Of note, as the number of recall hits and recall misses in the encoding task was not balanced (min 5–max 18 recall hits per participant out of a total of 60 figures), for each participant a subset of the recall misses were randomly selected, resulting in a matched number of trials for recall hits and misses. Similarly, as participants performed better than chance (50%) in the recognition task, the encoding task contained more recognition hits compared to misses. Thus, for each participant a subset of recognition hits was randomly selected, resulting in an equal number of trials for recognition hits and misses.

As a next step, at the individual level parameters were estimated for the following comparisons (in the following referred to as “contrasts”): Encoding task: subsequent hits > misses (indicative of ‘encoding success’ as defined in Spaniol et al. [35]); Recognition task: hits > correct rejections (with hits = correctly recognized old figures, correct rejections = correctly classified new figures; the contrast is indicative of ‘retrieval success’ as applied by Spaniol et al. [35]). In more detail, for the encoding task, two analyses were conducted (1) the model included the presentation onsets of figures correctly recalled later (subsequently referred to as “recall hits”) and of figures that were not recalled later (“recall misses”), (2) the model contained the onset times of figures correctly recognized later (“recognition hits”) and of figures not recognized later (“recognition misses”).

Subsequently, the resulting contrast images were submitted to a one-sample *t*-test across all participants to assess neuronal activations related to memory processing (“encoding success” and “retrieval success”) in general. Moreover, contrast images were entered in a random effects group analysis (ANOVAs with factor group: CO/IO/AIR, followed by *t*-contrasts). Whole-brain statistical maps were thresholded at $p < 0.001$ (uncorrected) and significance was examined at the cluster level, applying a statistical threshold of $p < 0.05$ and family-wise error

(FWE) correction. The coordinates of resulting activations are presented in MNI space. Main clusters of the networks and activation differences were labeled using the AAL toolbox [39].

2.2.6.4. Postprocessing fMRI data: group independent component analysis (ICA). After preprocessing of the functional data, group ICA [40] was performed for both tasks (encoding and recognition) separately using the GIFT toolbox (<http://icatb.sourceforge.net>). Before the data were submitted to ICA, data dimensions were reduced using principal component analysis (PCA). In two steps, the data were reduced to 60 and subsequently 45 (encoding)/91 and 66 (recognition) components. For each task, the optimal number of spatially independent networks was determined applying a modified minimum description length algorithm (MDL) implemented in the toolbox. For a more robust component estimation and assessment of the consistency of components, the ICASSO algorithm implemented in GIFT was used to repeat the analysis 20 times. The group ICA resulted in spatial maps of the functional networks and their associated time-courses. These components were compared visually and by means of spatial correlations to functional networks in a previous large-scale study [41]. Artfactual components (e.g. those exhibiting substantial spatial overlap with motion, susceptibility or ventricular artifacts) were excluded (see Table S3). The remaining components were subdivided, according to the classification proposed in Allen et al. [22], as subcortical, cognitive, cerebellar, default mode, visual, auditory, and somatosensory components. As the focus of the present study was on cognitive and olfactory networks, auditory, visual, and somatosensory components were not included in further analyses (see Table S3).

In a next step, we analyzed whether the component time courses were associated with stimulus presentation onsets of the paradigm. From a multiple regression of the time courses with participants’ design matrices including presentation times, beta weights were obtained for regressors of interest. For the encoding task, two different multiple regressions were conducted with different models: (1) model included the onsets of figures correctly recalled later (recall hits) and of figures that were not recalled later (recall misses) and (2) models included the onsets of figures correctly recognized (recognition hits) and of figures not recognized (recognition misses) subsequently. For both multiple regressions, six realignment parameters were additionally included as regressors of no interest. The design matrices for the multiple regression on the recognition task data included the onsets of hits, false alarms, correct rejections and misses of the recognition paradigm and six realignment parameters. The resulting beta weights of the regressors of interest (hits and correct rejections) indicated the degree to which the time course of each regressor was related to the time course of each neuronal component. Beta-weights were statistically compared between the groups by means of ANOVA (encoding task: factors were odor group and encoding success [hits/misses]; recognition task: factors were odor group and retrieval success [hits/correct rejections]). In case of a significant main effect of odor group, these were followed by three ANOVA, each comparing two of the groups to evaluate which groups were significantly different. In case of a significant main effect of encoding/retrieval success, we conducted paired *t*-tests (hits vs. misses or hits vs. correct rejections) across the whole sample. Additionally, one-sample *t*-tests on the beta weights of each trial type (hits and misses for the encoding task, hits and correct rejections for the recognition task) were conducted for the groups to assess whether component time courses were modulated by stimulus presentation onsets.

3. Results

3.1. Behavioral results

The three odor groups did not differ in the number of recalled figures in the free recall task, or in memory performance during the picture recognition task, with comparable hit rates, false alarm rates, d' , β

Table 1
Performance of the Free Recall and Recognition tasks by odor group.

	Free Recall No. correctly recalled	Recognition Task							
		Hit rate	FA rate	d'	β	Reaction time [s]			
						Hits	FA	Correj	Misses
CO	9.82 (2.34)	0.71 (0.09)	0.17 (0.08)	1.61 (0.38)	1.57 (0.71)	1.50 (0.31)	1.90 (0.47)	1.46 (0.31)	1.85 (0.45)
IO	10.04 (3.38)	0.74 (0.10)	0.18 (0.11)	1.66 (0.47)	1.48 (0.74)	1.41 (0.18)	1.74 (0.46)	1.44 (0.28)	1.93 (0.43)
AIR	10.88 (3.12)	0.71 (0.12)	0.20 (0.10)	1.49 (0.44)	1.47 (1.04)	1.42 (0.17)	1.65 (0.40)	1.49 (0.35)	1.83 (0.50)

Hit rate calculated as hits/no. of all targets; FA rate = false alarm rate [calculated as no. of false alarms/no. of all non-targets]; d' and β calculated according to Tables 1 and 2 in [33]. Free recall performance is number correctly recalled out of 60 stimuli. Correj = correct rejections; CO = congruent odor group; IO = incongruent odor group; AIR = control group receiving odorless air. All data shown as mean (standard deviation).

and reaction times (see Table 1; $p > 0.1$ for all between-group comparisons). The additional analysis of recognition performance after removing the recalled items did not result in group differences in hit rates, d' or β either (see Table S2). A comparison of the ratings from the CO and IO group after the recognition task indicated that mean scores for intensity (CO 6.7 vs. IO 6.8), pleasantness (5.8 vs. 4.9), familiarity (7.2 vs. 7.4), and invigorating quality (4.9 vs. 5.3) of the presented odor (lavender or vanilla, respectively) did not differ between the two groups; all $p > 0.1$ in two-sample *t*-tests. Moreover, there were no group differences in mood or affective state throughout the experiment (see Figs. S3 and S4; for main effect group and interactions all $p > 0.4$).

3.2. Imaging results: brain activation during successful picture encoding

3.2.1. GLM results

As described in section 2.2.6, we analyzed brain activation during successful picture encoding by comparing trials which were successfully recognized or recalled later (subsequent hits) to trials which were not (subsequent misses). Successful encoding as defined by subsequent correct recognition (contrast recognition hits > recognition misses) was accompanied by activation in the inferior frontal gyrus, inferior occipital gyrus, superior parietal gyrus, and inferior temporal gyrus (see Table 2 and Appendix BFig. S1). No significant differences were observed between odor groups for this contrast.

Successful encoding as defined by subsequent correct recall (contrast recall hits > recall misses) was accompanied by activation in the inferior frontal gyrus, largely overlapping with the activations observed for recognition hits > misses (see Table 2 and Appendix BFig. S1). Comparison of CO > IO (for hits > misses) revealed a significant cluster in the region of the piriform cortex (see Fig. 2 and Table 2). As

the piriform cortex is not included in most standard brain atlases, for further characterization the activation was compared to piriform cortex activity (see Fig. 2) reported in the literature (meta-analysis of olfactory studies, Seubert et al. [42]). No other significant between-group differences were observed.

3.2.2. ICA results

Functional networks showing a significant modulation by encoding success (subsequent hits/misses) or between the groups are presented in Fig. 3, see Appendix BTable S4 for a list of the brain regions included in the spatial maps of the components. Several networks showed differential modulation for recognition hits and misses, as reflected by a significant main effect of encoding success: This was the case for two default mode network (DMN) components: EC14: $F(1,96) = 5.55$, $p = 0.02$; EC43: $F(1,96) = 8.93$, $p < 0.01$, resulting from a stronger negative task-modulation for subsequent hits compared to misses (see Fig. 3). One cognitive control (CC) network, EC23: $F(1,96) = 16.53$, $p < 0.01$ showed a stronger positive modulation for subsequent hits compared to misses, while the opposite pattern (more positive modulation for misses compared to hits) was observed for another CC, EC28: $F(1,96) = 4.08$, $p = 0.046$ (see Fig. 3).

For subsequent recall hits and misses, EC14 and EC23 showed the same pattern of task-modulation as for recognition hits/misses: EC14: $F(1,96) = 4.62$, $p = 0.03$; EC23: $F(1,96) = 17.99$, $p < 0.01$ (see Fig. 3). Furthermore, task-modulation for one DMN, EC20, differed between odor groups ($F(2,96) = 4.2$, $p = 0.02$), with greater negative task-modulation for AIR versus IO (main effect group: $F(1,64) = 7.65$, $p = 0.01$), while the difference did not reach significance for AIR versus CO (main effect group: $F(1,64) = 3.54$, $p = 0.06$).

Table 2
Significant clusters of neuronal activation during the encoding task.

Brain region	Side	Cluster size	Peak MNI coordinates			Peak T-value	p-value (peak-level unc.)	p-value (cluster-level FWE-corr.)	k (cluster size)
			x	y	z				
Recognition Hits > Misses^a									
Inferior occipital gyrus, inferior temporal gyrus	L	4210	-46	-52	-12	6.22	0.000	0.000	4210
Inferior frontal gyrus, triangular part and opercular part	R	2674	46	8	28	5.90	0.000	0.000	2674
Inferior frontal gyrus, triangular part	L	5504	-45	4	32	5.87	0.000	0.000	5504
Superior parietal gyrus	L	5453	-22	-62	48	5.76	0.000	0.000	5453
Inferior temporal gyrus	R	7756	46	-51	-10	5.45	0.000	0.000	7756
Recall Hits > Misses^a									
Inferior frontal gyrus, triangular part	L	1545	-51	30	12	4.14	0.000	0.002	1545
CO > IO for Recall Hits > Misses									
Piriform cortex	L	873	-24	6	0	4.40	0.000	0.021	873

^a One-sample *t*-test across all participants. Only clusters significant at a cluster level threshold of $p < 0.05$ with family-wise error (FWE) correction are presented. CO = congruent odor group, IO = incongruent odor group. MNI = Montreal Neurological Institute. L = left, R = right. See also Fig. S1.

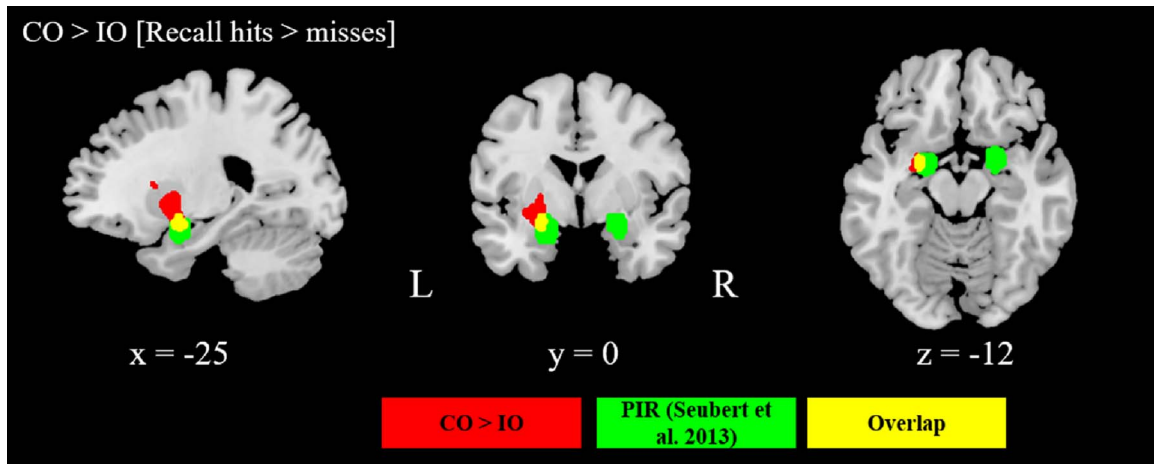


Fig. 2. Task-modulation during encoding: CO > IO (For interpretation of the references to colour in this figure legend, the reader is referred to the web version of this article.). Significant cluster (cluster-level FWE-corr $p < 0.05$) for the CO versus IO group for recall hits > recall misses during the encoding task (red areas). For comparison the green areas show piriform cortex activation previously reported in the literature on a meta-analysis of olfactory studies (Seubert et al. [42]).

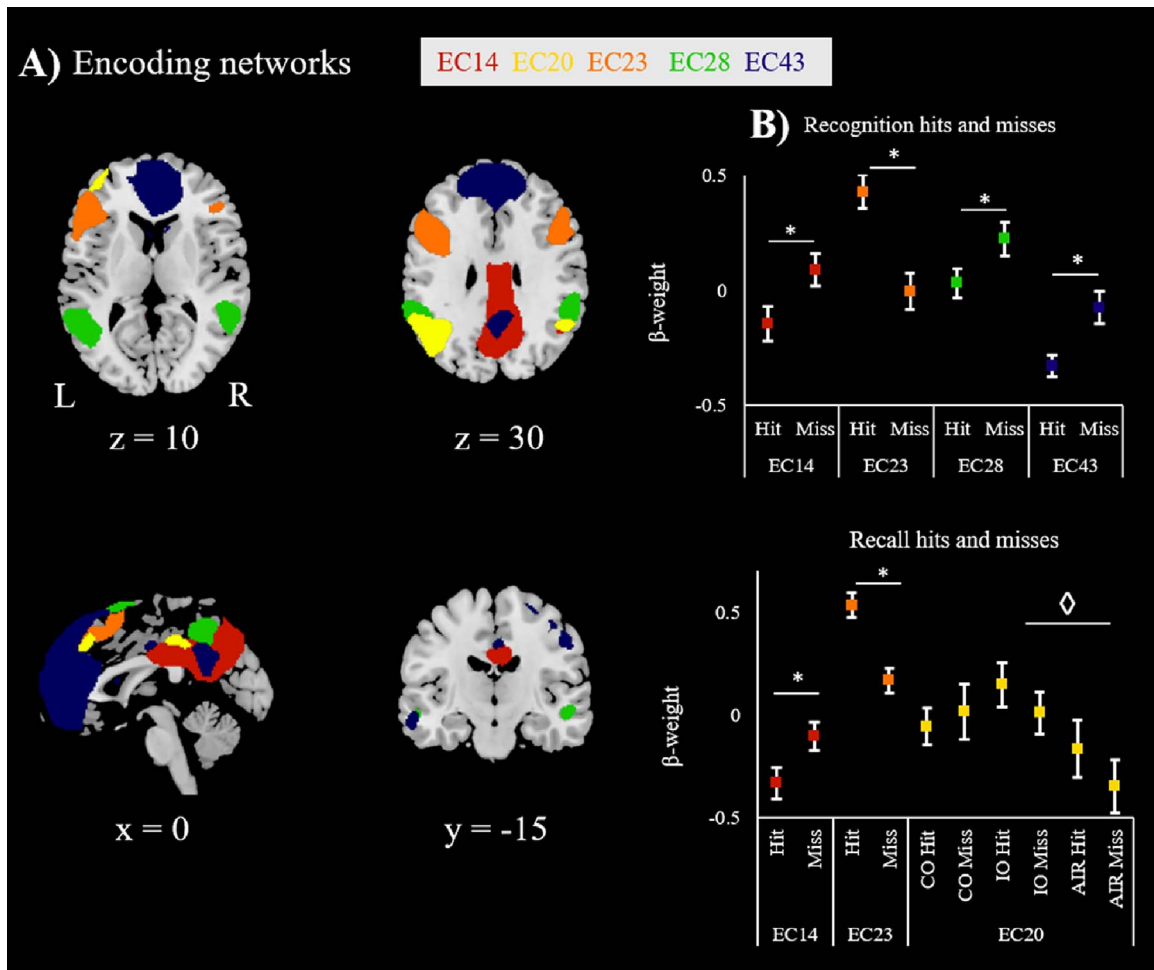


Fig. 3. Task-modulation during encoding. (A) Spatial maps of the brain components that showed differential modulation by hits versus misses or between groups during the encoding task. Height threshold for all maps $p < 1 \times 10^{-12}$, FDR. (B) Beta weights of the respective components for each trial type (hit/miss), for trials classified according to subsequent recognition or recall performance. *Significant difference in beta weights between trial types at $p < 0.05$ (paired t -test across all participants) \diamond significant difference of beta weights between groups at $p < 0.05$ (two-group ANOVA between respective groups, main effect group).

Table 3
Significant clusters of activation during retrieval success (OneST hits > correct rejections) in the recognition task.^a

Brain region (Peak/nearest grey matter)	Side	Cluster size	Peak MNI coordinates			Peak T-value	p-value (peak-level FWE-corrected)
			x	y	z		
Insula_L	L	1676	-33	20	-3	10.65	0.000
Frontal_Sup_Medial_L	L	2307	-2	28	38	10.23	0.000
Cuneus_L	L	17763	-4	-69	28	10.12	0.000
Caudate_L	L	3078	-8	14	6	9.64	0.000
Frontal_Mid_L	L	2922	-33	52	4	8.85	0.000
Frontal_Mid_L	L	3025	-48	24	36	8.47	0.000
Frontal_Mid_R	R	500	28	9	52	7.35	0.000
Cerebellum_7b_R	R	207	33	-68	-48	7.16	0.000
Cingulum_Mid_L	L	459	0	-26	34	7.10	0.000
Cerebellum_6_R, Cerebellum_Crus1_R	R	227	33	-63	-26	7.16	0.000
Thalamus_L							
Hippocampus_L	L	207	-22	-27	-2	6.89	0.000
Insula_R	R	260	33	24	-4	6.75	0.000
Lingual_L	L	1117	-10	-81	-10	6.58	0.001
Frontal_Mid_L	L	458	-38	6	62	6.33	0.002
Frontal_Inf_Oper_L	L	186	-50	16	12	6.21	0.002
Cerebellum_Crus1_R, Cerebellum_6_R	R	129	10	-76	-26	6.16	0.003
Temporal_Mid_R	R	131	57	-48	-8	6.15	0.003
Frontal_Mid_R	R	326	44	36	20	6.02	0.004

^a Only activations significant at a height-level threshold of $p < 0.05$ with family-wise error (FWE) correction and $k > 100$ are presented. OneST = One-sample *t*-test across all participants. CO = congruent group, IO = incongruent group. MNI = Montreal Neurological Institute. L = left, R = right. Brain regions were labelled using the AAL (automatic anatomical labelling) atlas (<http://www.gin.cnrs.fr/AAL?lang=en>) [39] as included in the xjView toolbox (<http://www.alivelearn.net/xjview>). See also Appendix BFig. S2.

3.3. Imaging results: recognition task

3.3.1. GLM results

Across all participants, several brain regions (including the insula, cerebellum, caudate nucleus, cingulum, thalamus, and hippocampus) showed more activation during hits than during correct rejections (see Table 3 and Appendix BFig. S2). The opposite contrast (correct rejections > hits) did not result in any significant activations. There were no significant differences in activation between the odor groups for these contrasts.

3.3.2. ICA results

Components showing a differential task-modulation depending on retrieval success (hits versus correct rejections) or between the odor groups are shown in Fig. 4 and Fig. 5, see Appendix ATable S5 for a list of the brain regions included in spatial maps of the components. Two subcortical components showed differential modulation between the groups: RC32: $F(2,96) = 4.76$, $p = 0.01$ and RC35: $F(2,96) = 3.997$, $p = 0.02$. RC32 was positively modulated to a greater extent for IO as compared to CO ($F(1,64) = 8.59$, $p = 0.01$) and AIR ($F(1,64) = 4.6$, $p = 0.04$) [see Fig. 4]. This was also the case for RC35 (IO vs. CO: $F(1,64) = 5.62$, $p = 0.02$; IO vs. AIR: $F(1,64) = 6.18$, $p = 0.02$). Additionally, RC35 showed stronger positive task-modulation for hits versus correct rejections ($F(1,96) = 23.97$, $p < 0.01$); this was also the case for component RC41 ($F(1,96) = 5.68$, $p = 0.02$) [see Fig. 4].

As shown in Fig. 5, four DMN components showed differential task-modulation for hits versus correct rejections: RC33: $F(1,96) = 4.9$, $p = 0.03$; RC34: $F(1,96) = 7$, $p < 0.01$; RC45: $F(1,96) = 20.64$, $p < 0.01$; RC52: $F(1,96) = 18.65$, $p < 0.01$; RC66: $F(1,96) = 5.7$, $p = 0.02$, with more reduced positive task-modulation in RC33, and stronger negative task-modulation in the remaining three DMN, for correct rejections versus hits. Four CC components also showed differences in task-modulation between hits and correct rejections: RC47 ($F(1,96) = 9.37$, $p < 0.01$); RC55 ($F(1,96) = 18$, $p < 0.01$); RC58 ($F(1,96) = 24$, $p < 0.01$); RC62 ($F(1,96) = 4$, $p = 0.047$). In all cases, there was a stronger positive task-modulation for hits versus correct rejections (see Fig. 5).

4. Discussion

By using odor contexts during fMRI scanning, the present study extends previous purely behavioral research on context-dependent memory effects. Subjects participated in an incidental picture encoding task during fMRI, a free recall task and a yes/no recognition fMRI task, while congruent or incongruent odors were presented as contextual cues. No differences in behavioral memory performance (picture recognition/recall) were observed between the CO, IO or control groups, while we demonstrated that odor contexts influence neuronal memory-related processes.

As a proof-of-principle of our paradigms and to enable comparison with previous memory studies, we first analyzed the pattern of brain activation during successful picture encoding across all participants. As a recognition task and a free recall task were performed, two types of encoding success were analyzed: Encoding success as defined by correct recognition and encoding success defined by correct recall of the presented items. Results revealed that across the whole sample, subsequent correct *recognition* (compared to failure of recognition) was primarily associated with activation within the inferior occipital, inferior temporal and inferior frontal gyrus and superior parietal gyrus. This finding is in accordance with activation patterns associated with encoding success in a meta-analysis of event-related fMRI studies [35]. While the meta-analysis found the greatest concordance of activations in the left hemisphere, we observed bilateral activations in our study. This might reflect the type of stimulus used: most previous studies used verbal material, thus verbal processing may have contributed to the left-sided activation pattern observed. In the present study abstract line drawings were encoded, possibly contributing to the bilateral activations. In general, subsequent correct *recall* (versus failure of recall) was characterized mainly by activation in the left inferior frontal gyrus (pars triangularis). Thus, deeper processing (leading to later recall) was particularly related to activation within the inferior frontal gyrus, a region previously linked to semantic and phonological processing [43,44]. In line with the 'levels-of-processing' framework [45,46], these results suggest that pictures evoking stronger semantic associations led to a deeper memory encoding and subsequent better recall performance.

Intriguingly, the CO group showed increased activation of the piriform cortex during successful encoding of stimuli, compared to the

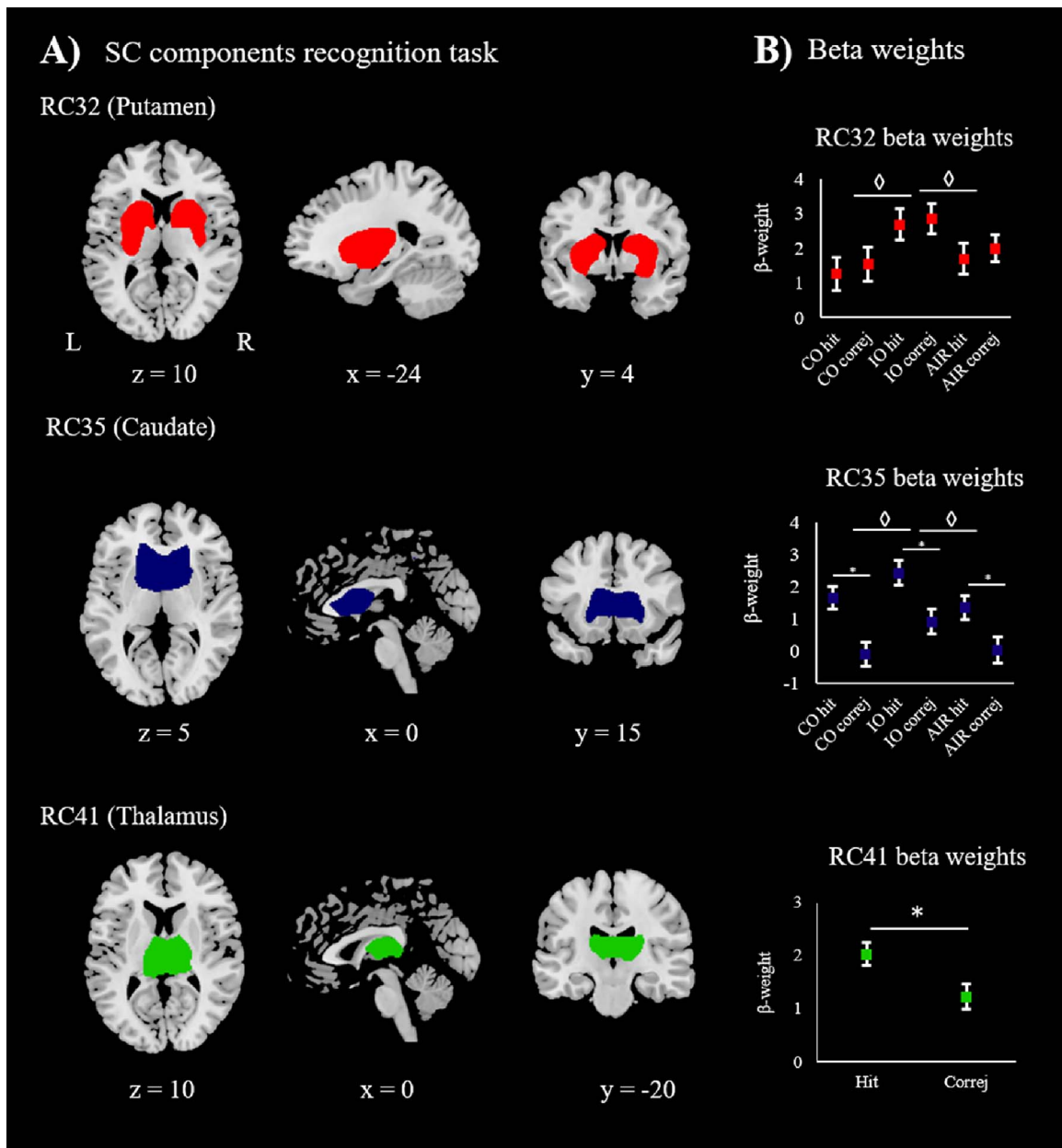


Fig. 4. Task-modulation of subcortical (SC) components during the recognition task. (A) Spatial maps of SC components showing differences in beta weights between groups or for hits versus correct rejections (correj) during the recognition task. Height threshold for all maps $p < 1 \times 10^{-12}$, FDR. (B) Beta weights of the respective components for hits and correct rejections (correj). *Significant difference of beta weights between trial types (hits/correj) at $p < 0.05$ (paired *t*-test) \diamond significant difference off beta weights between groups at $p < 0.05$ (two-group ANOVA, main effect group).

IO group. A tentative explanation for this finding might be that the congruent odor context led to enhanced recall of stimuli that were integrated with an olfactory percept for CO. Thus, we speculate that the congruent odor served as a retrieval cue for CO, evoking the recall of primarily those figures that were associated with the odor during encoding. This supports previous data suggesting that the piriform cortex is essential for integrating olfactory input and higher-order information [47–49]. In general, this finding is in line with our expectations of an integration of olfactory context cue and figural stimuli during successful encoding. However, as discussed below, in our study no effect of odor context on behavioral memory performance was visible. Thus, to confirm whether this finding is reflective of differences in neurocognitive processing caused by the odor context cues, future studies optimized to reveal stronger context-dependent effects are required. Moreover, as we only used two odors in the present study, future studies are needed to

elucidate the generalizability of our findings with different odors and types of encoded information. In particular, the question whether there are interactions between the type of encoded stimulus (i.e., figures, faces, words) and the type of odors used as contextual cues (such as social or food-related odors etc.) might be of interest.

In addition to GLM-based analyses, we performed ICA to study functional networks and assess their modulation during the encoding memory task. In the encoding task, the DMN and the CC networks in particular showed differential task-modulation in all three odor groups. For stimuli that were successfully encoded, deactivation of the DMN was apparent, in line with previous studies showing decreases in DMN activation during attention-demanding tasks [50,51]. As suggested previously, and consistent with neuroimaging findings [52], DMN activity might reflect mind-wandering and deflection of task-related attention. A CC network (EC23) comprising the middle frontal gyrus

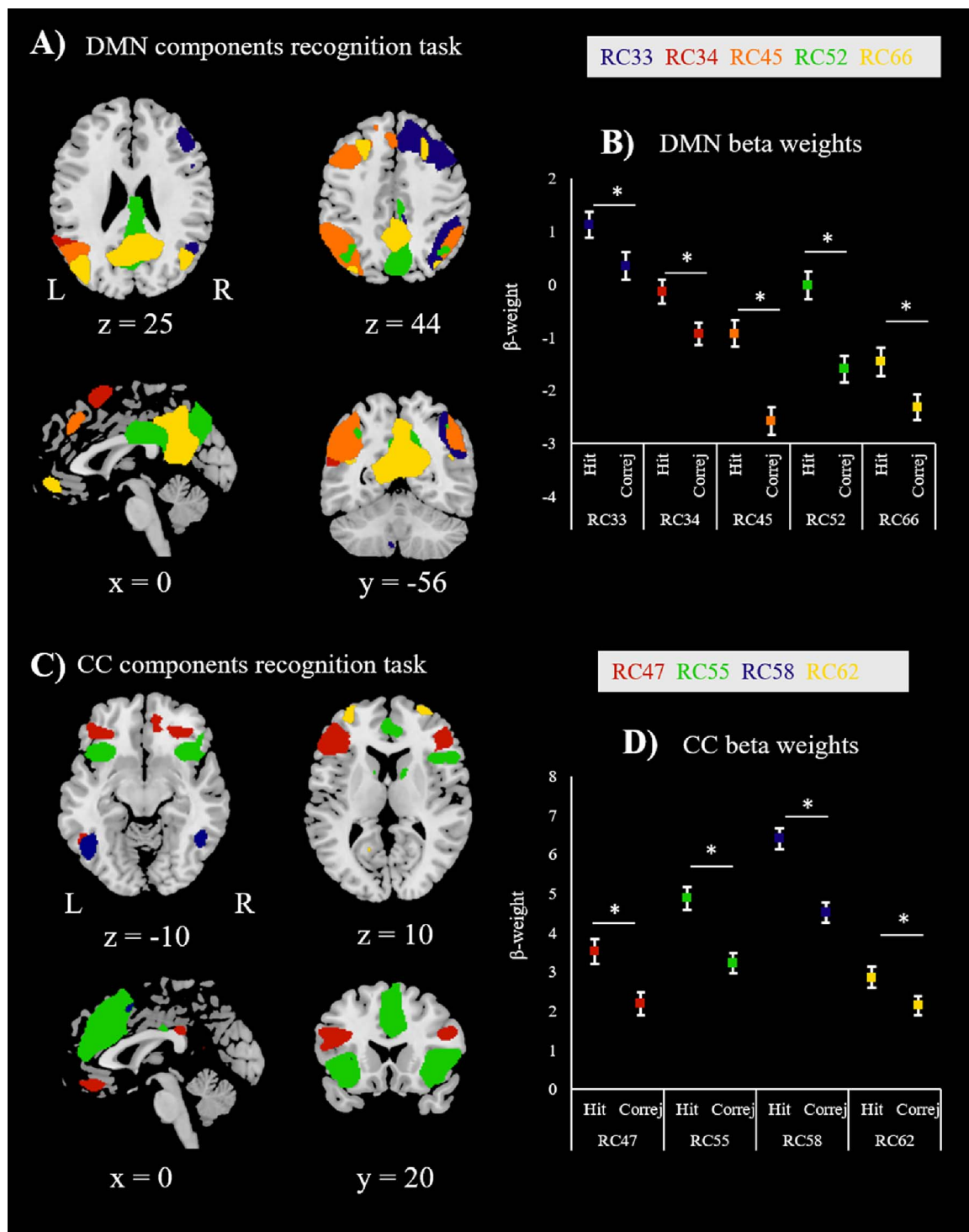


Fig. 5. Task-modulation of default mode network (DMN) and cognitive control (CC) components during the recognition task. (A) Spatial maps of the DMN components showing differential modulation by hits and correct rejections (correj) during the recognition task (height threshold for all maps $p < 1 \times 10^{-12}$, FDR). (B) Beta weights of the respective DMN components for each trial type (hits and correj). *Significant differences at $p < 0.05$ (paired *t*-test across all participants). (C) Spatial maps of the CC components showing differential modulation by hits and correct rejections (correj) during the recognition task (height threshold for all maps $p < 1 \times 10^{-12}$, FDR). (D) Beta weights of the respective CC components for each trial type (hits and correj), *significant differences at $p < 0.05$ (paired *t*-test across all participants).

showed increased task-modulation during successful encoding, consistent with previous investigations linking this region to intrinsic alertness [53]. Furthermore, activity in the left inferior frontal gyrus is involved in visuo-perceptual working memory processing [16]. Another part of the CC network, EC28, showed the opposite pattern, with increased task-modulation during subsequent recognition misses as

compared to hits. A closer look at the areas comprised in the spatial map of this network indicated that EC28 also showed substantial spatial overlap with regions considered to be part of the DMN, such as the precuneus. For recall hits versus misses, EC14 and EC23 showed the same pattern as for recognition hits versus misses. Additionally, EC20, a part of the DMN comprising left inferior parietal gyrus, angular gyrus

and middle frontal gyrus showed a stronger negative task-modulation in the AIR group in comparison with IO, and the same tendency for AIR compared to CO. The stronger deactivation of this component in the no-odor group (irrespective of retrieval success) might reflect a stronger focus on the task by this group. However, as other parts of the DMN did not show these group differences, this finding should be interpreted with caution.

Across the whole sample, increased activation for successful retrieval (hits > correct rejections) was observed particularly in areas such as the medial frontal gyrus, insula, cuneus, and caudate nucleus, primarily on the left side. These regions overlap almost completely with those reported in the meta-analysis of event-related memory MRI studies [35], although the activations that we observed in the caudate nucleus, insula, hippocampus, thalamus, and inferior frontal gyrus were more pronounced. As the caudate nucleus, insula, hippocampus, and thalamus in particular play important roles in olfactory perception, a potential explanation for this finding might be that recognition of figures evoked a reactivation of these olfactory processing areas. This would concur with a previous report that when pictures were paired with odors during encoding, successful retrieval was accompanied by activation in olfactory areas when pictures were presented without odor [54]. However, as our study did not include a group receiving an odor during encoding, but not during retrieval, comparability to this study remains limited. Moreover, Gottfried et al. [54] observed re-activation mainly within the piriform cortex and hippocampus, but not in the insula, caudate nucleus or thalamus.

Group ICA also revealed group differences in the recruitment of functional networks during the recognition task: IO showed a stronger positive task-modulation within two subcortical networks (putamen and caudate) compared to CO and AIR. This result indicates that the two odors that we used (lavender and vanilla) were processed differently, despite their highly similar ratings for pleasantness, intensity and familiarity. This pattern of distinct group differences confirms that ICA can reveal additional information not uncovered by traditional model-driven analyses. Hits and correct rejections were mainly characterized by differential recruitment of CC and DMN components. CC networks, comprising mainly the insula, middle and inferior frontal gyrus, and inferior parietal lobule, were consistently activated more strongly by hits than by correct rejections, in line with previous studies employing higher-order cognitive tasks [55–57]. Moreover, the DMN consistently showed a stronger deactivation (or weaker activation in the case of RC33) for correct rejections. These results extend previous findings, in particular on a deactivation of anterior parts of the DMN during episodic memory retrieval [58]. Two subcortical components, the caudate nucleus and thalamus, were also task-modulated differentially for hits and correct rejections, underscoring previous tentative evidence that subcortical structures might play a role in episodic memory function [59].

In the present study, congruent odor contexts did not lead to enhanced picture retrieval. It is possible that the noisy and demanding environment of the MRI scanner might have overshadowed the effects of odors presented during the encoding task (see also [60] for a discussion of “overshadowing” processes). Previous studies suggest that the distinctiveness of ambient odors against the contextual background plays an important role in the emergence of context-dependent memory effects [6]. Thus, the MRI context itself in our study might have been more important than the presented odors. Moreover, the MRI environment might have increased participants’ stress levels [61,62]. As a previous study indicates that stress can disrupt context-dependent memory effects [4], including a mock scanner session or including only MRI-experienced participants might enable stronger context-dependent memory effects. However, as another recent study reported that odors can serve as retrieval cues for memories of stressful episodes [10], the relation between stress experience and context-dependent memory effects remains to be investigated in more detail. Future studies might also elucidate whether a stronger context-dependent memory effect

occurs if only the recognition task is carried out in the scanner, while encoding takes place in a less distracting and stressful environment, for instance in a scented room.

In conclusion, we did not find an enhancement of memory performance when pictures were presented in a congruent odor context during encoding and retrieval. However, the congruent odor was associated with increased activation in the piriform cortex during successful encoding, while the incongruent odor was associated with stronger task-modulation within subcortical networks during recognition. Overall, our results shed more light on the recruitment of functional neuronal networks during picture encoding and recognition, and pave the way for future investigations of the impact of odor contexts on cognitive performance.

Author contributions

Conceptualization and Experimental Design: J.R., M.N., W.S., V.S.; Data Acquisition: J.R., C.H., D.B.; Analysis: J.R., C.H.; D.B.; Project supervision: V.S.; Drafting of the Manuscript: J.R., V.S.; Review & Editing of the Manuscript: J.R., M.N., W.S., C.H., D.B., V.S.

Acknowledgements

Manuel Ninaus was supported by the Leibniz-Competition Fund (SAW-2016-IWM-3). We would like to thank Heimbs (Braunschweig, Germany) for providing products for subject compensation, aromainfo.at for providing the diffusor and IFF (New York, USA, <http://www.iff.com/>) for providing several odors used in the pre-study. Furthermore we thank Jennifer Kern, Vanessa Hinterleitner and Bettina Brückler for help during data acquisition and analysis. We would also like to thank Jessica Freiherr for discussions and input on study conceptualization. Julia Balfour of Northstar Medical Writing and Editing Services provided English-language editing support. The authors declare no conflicts of interest.

Appendix A. Supplementary data

Supplementary data associated with this article can be found, in the online version, at <http://dx.doi.org/10.1016/j.bbr.2017.06.022>.

References

- [1] J. Willander, M. Larsson, Smell your way back to childhood: autobiographical odor memory, *Psychon. Bull. Rev.* 13 (2006) 240–244, <http://dx.doi.org/10.3758/BF03193837>.
- [2] R. Herz, J. Schooler, A naturalistic study of autobiographical and visual evoked by olfactory memories the Proustian cues: testing hypothesis, *Am. J. Psychol.* 115 (2002) 21–32, <http://dx.doi.org/10.2307/1423672>.
- [3] S. Chu, J.J. Downes, Proust nose best: odors are better cues of autobiographical memory, *Mem. Cognit.* 30 (2002) 511–518, <http://dx.doi.org/10.3758/BF03194952>.
- [4] L. Schwabe, A. Böhringer, O.T. Wolf, Stress disrupts context-dependent memory, *Learn. Mem.* 16 (2009) 110–113, <http://dx.doi.org/10.1101/lm.1257509>.
- [5] L.J. Ball, J. Shoker, J.N.V. Miles, Odour-based context reinstatement effects with indirect measures of memory: the curious case of rosemary, *Br. J. Psychol.* 101 (2010) 655–678, <http://dx.doi.org/10.1348/000712609X479663>.
- [6] R.S. Herz, The effects of cue distinctiveness on odor-based context-dependent memory, *Mem. Cognit.* 25 (1997) 375–380, <http://dx.doi.org/10.3758/BF03211293>.
- [7] A. Parker, A. Gellatly, Moveable cues: a practical method for reducing context-dependent forgetting, *Appl. Cogn. Psychol.* 11 (1997) 163–173, [http://dx.doi.org/10.1002/\(SICI\)1099-0720\(199704\)11:2<163::AID-ACP427>3.0.CO;2-1](http://dx.doi.org/10.1002/(SICI)1099-0720(199704)11:2<163::AID-ACP427>3.0.CO;2-1).
- [8] A. Parker, H. Ngu, H.J. Cassaday, Odour and proustian memory reduction of context-dependent forgetting and multiple forms of memory, *Appl. Cogn. Psychol.* 15 (2001) 159–171, [http://dx.doi.org/10.1002/1099-0720\(200103/04\)15:2<159::AID-ACP694>3.0.CO;2-D](http://dx.doi.org/10.1002/1099-0720(200103/04)15:2<159::AID-ACP694>3.0.CO;2-D).
- [9] D.G. Smith, L. Standing, A. de Man, Verbal memory elicited by ambient odor, *Percept. Mot. Ski.* 74 (1992) 339–343, <http://dx.doi.org/10.2466/PMS.74.2.339-343>.
- [10] U.S. Wiemers, M.M. Sauvage, O.T. Wolf, Odors as effective retrieval cues for stressful episodes, *Neurobiol. Learn. Mem.* 112 (2014) 230–236, <http://dx.doi.org/10.1016/j.nlm.2013.10.004>.
- [11] F.R. Schab, Odors and the remembrance of things past, *J. Exp. Psychol. Learn. Mem. Cogn.* 16 (1990) 648–655, <http://dx.doi.org/10.1037/0278-7393.16.4.648>.

- [12] D.A. Wilson, A.R. Best, R.M. Sullivan, Plasticity in the olfactory system: lessons for the neurobiology of memory, *Neuroscientist* 10 (2004) 513–524, <http://dx.doi.org/10.1016/j.biotechadv.2011.08.021>.
 [13] A.-L. Saive, J.-P. Royet, J. Plailly, A review on the neural bases of episodic odor memory: from laboratory-based to autobiographical approaches, *Front. Behav. Neurosci.* 8 (2014) 1–13, <http://dx.doi.org/10.3389/fnbeh.2014.00240>.
 [14] M.D. Rugg, K.L. Vilberg, J.T. Mattson, S.S. Yu, J.D. Johnson, M. Suzuki, Item memory, context memory and the hippocampus: fMRI evidence, *Neuropsychologia* 50 (2012) 3070–3079, <http://dx.doi.org/10.1016/j.neuropsychologia.2012.06.004>.
 [15] K. Il Dae, D.S. Manoach, D.H. Mathalon, J.A. Turner, M. Mannell, G.G. Brown, J.M. Ford, R.L. Gollub, T. White, C. Wible, A. Belger, H.J. Bockholt, V.P. Clark, J. Lauriello, D. O'Leary, B.A. Mueller, K.O. Lim, N. Andreasen, S.G. Potkin, V.D. Calhoun, Dysregulation of working memory and default-mode networks in schizophrenia using independent component analysis, an fBIRN and MCIC study, *Hum. Brain Mapp.* 30 (2009) 3795–3811, <http://dx.doi.org/10.1002/hbm.20807>.
 [16] R. Sala-Llonch, E.M. Palacios, C. Junqué, N. Bargalló, P. Vendrell, Functional networks and structural connectivity of visuospatial and visuosperceptual working memory, *Front. Hum. Neurosci.* 9 (2015) 340, <http://dx.doi.org/10.3389/fnhum.2015.00340>.
 [17] G.E. van den Bosch, H. El Marroun, M.N. Schmidt, D. Tibboel, D.S. Manoach, V.D. Calhoun, T.J.H. White, Brain connectivity during verbal working memory in children and adolescents, *Hum. Brain Mapp.* 35 (2014) 698–711, <http://dx.doi.org/10.1002/hbm.22193>.
 [18] E. Saliassi, L. Geerlings, M.M. Lorist, N.M. Maurits, Neural correlates associated with successful working memory performance in older adults as revealed by spatial ICA, *PLoS One* 9 (2014) e99250, <http://dx.doi.org/10.1371/journal.pone.0099250>.
 [19] J. Xu, S. Zhang, V.D. Calhoun, J. Monterosso, C.S.R. Li, P.D. Worhunsky, M. Stevens, G.D. Pearlson, M.N. Potenza, Task-related concurrent but opposite modulations of overlapping functional networks as revealed by spatial ICA, *Neuroimage* 79 (2013) 62–71, <http://dx.doi.org/10.1016/j.neuroimage.2013.04.038>.
 [20] T. Iidaka, A. Matsumoto, J. Nogawa, Y. Yamamoto, N. Sadato, Frontoparietal network involved in successful retrieval from episodic memory. Spatial and temporal analyses using fMRI and ERP, *Cereb. Cortex* 16 (2006) 1349–1360, <http://dx.doi.org/10.1093/cercor/bhl040>.
 [21] K. a. Celone, V.D. Calhoun, B.C. Dickerson, A. Atri, E.F. Chua, S.L. Miller, K. DePeau, D.M. Rentz, D.J. Selkoe, D. Blacker, M.S. Albert, R. a. Sperling, Alterations in memory networks in mild cognitive impairment and Alzheimer's disease: an independent component analysis, *J. Neurosci.* 26 (2006) 10222–10231, <http://dx.doi.org/10.1523/JNEUROSCI.2250-06.2006>.
 [22] E.A. Allen, E.B. Erhardt, Y. Wei, T. Eichele, V.D. Calhoun, Capturing inter-subject variability with group independent component analysis of fMRI data: a simulation study, *Neuroimage* 59 (2012) 4141–4159, <http://dx.doi.org/10.1016/j.neuroimage.2011.10.010>.
 [23] M.J. McKeown, S. Makeig, G.G. Brown, T.-P. Jung, S.S. Kindermann, A.J. Bell, T.J. Sejnowski, Analysis of fMRI data by blind separation into independent spatial components, *Hum. Brain Mapp.* 6 (1998) 160–188, [http://dx.doi.org/10.1002/\(SICI\)1097-0193\(1998\)6:3<160::AID-HBMS5>3.0.CO;2-1](http://dx.doi.org/10.1002/(SICI)1097-0193(1998)6:3<160::AID-HBMS5>3.0.CO;2-1).
 [24] J. Frasnelli, J.N. Lundström, V. Schöpf, S. Negoias, T. Hummel, F. Lepore, Dual processing streams in chemosensory perception, *Front. Hum. Neurosci.* 6 (2012) 288, <http://dx.doi.org/10.3389/fnhum.2012.00288>.
 [25] P. Karunanayaka, P.J. Eslinger, J.-L. Wang, C.W. Weitekamp, S. Molitoris, K.M. Gates, P.C.M. Molenaar, Q.X. Yang, Networks involved in olfaction and their dynamics using independent component analysis and unified structural equation modeling, *Hum. Brain Mapp.* 35 (2014) 2055–2072, <http://dx.doi.org/10.1002/hbm.22312>.
 [26] T. Hummel, B. Sekinger, S.R. Wolf, E. Pauli, G. Kobal, Sniffin sticks': olfactory performance assessed by the combined testing of odor identification, odor discrimination and olfactory threshold, *Chem. Senses* 22 (1997) 39–52.
 [27] T. Hummel, G. Kobal, H. Gudziol, A. Mackay-Sim, Normative data for the Sniffin' Sticks including tests of odor identification, odor discrimination, and olfactory thresholds: an upgrade based on a group of more than 3,000 subjects, *Eur. Arch. Oto-Rhino-Laryngology* 264 (2007) 237–243, <http://dx.doi.org/10.1007/s00405-006-0173-0>.
 [28] T. Nishimoto, T. Ueda, K. Miyawaki, Y. Une, M. Takahashi, A normative set of 98 pairs of nonsensical pictures (doodles), *Behav. Res. Methods* 42 (2010) 685–691, <http://dx.doi.org/10.3758/BRM.42.3.685>.
 [29] D. Watson, L.A. Clark, A. Tellegen, Development and validation of brief measures of positive and negative affect: the PANAS scales, *J. Pers. Soc. Psychol.* 54 (1988) 1063–1070, <http://dx.doi.org/10.1037/0022-3514.54.6.1063>.
 [30] S. Janke, A. Glöckner-Rist, Deutsche Version der Positive and Negative Affect Schedule (PANAS), *Zusammenstellung Sozialwissenschaftlicher Items Und.* (2014).
 [31] J.N. Lundström, A.R. Gordon, E.C. Alden, S. Boesveldt, J. Albrecht, Methods for building an inexpensive computer-controlled olfactometer for temporally-precise experiments, *Int. J. Psychophysiol.* 78 (2010) 179–189, <http://dx.doi.org/10.1016/j.ijpsycho.2010.07.007>.
 [32] K. Hallgren, Computing inter-rater reliability for observational data: an overview and tutorial, *Tutor. Quant. Methods Psychol.* 8 (2012) 23–24.
 [33] H. Stanislaw, N. Todorov, Calculation of signal detection theory measures, *Behav. Res. Methods Instruments Comput.* 31 (1999) 137–149.
 [34] J. Ashburner, A fast diffeomorphic image registration algorithm, *Neuroimage* 38 (2007) 95–113.
 [35] J. Spaniol, P.S.R. Davidson, A.S.N. Kim, H. Han, M. Moscovitch, C.L. Grady, Event-related fMRI studies of episodic encoding and retrieval: meta-analyses using activation likelihood estimation, *Neuropsychologia* 47 (2009) 1765–1779, <http://dx.doi.org/10.1016/j.neuropsychologia.2009.02.028>.
 [36] P. Reber, R. Siwiec, D. Gitleman, Neural correlates of successful encoding identified using functional magnetic resonance imaging, *J. Neurosci.* 22 (2002) 9541–9548.
 [37] L. Otten, R. Henson, M. Rugg, State-related and item-related neural correlates of successful memory encoding, *Nat. Neurosci.* 5 (2002) 1339–1344.
 [38] S. Brassens, W. Weber-Fahr, T. Sommer, J.T. Lehmbeck, D.F. Braus, Hippocampal–prefrontal encoding activation predicts whether words can be successfully recalled or only recognized, *Behav. Brain Res.* 171 (2006) 271–278, <http://dx.doi.org/10.1016/j.bbr.2006.04.002>.
 [39] N. Tzourio-Mazoyer, B. Landeau, D. Papathansassiou, F. Crivello, O. Etard, N. Delcroix, B. Mazoyer, M. Joliot, Automated anatomical labeling of activations in SPM using a macroscopic anatomical parcellation of the MNI MRI single-subject brain, *Neuroimage* 15 (2002) 273–289.
 [40] V.D. Calhoun, T. Adali, G.D. Pearlson, J.J. Pekar, A method for making group inferences from functional MRI data using independent component analysis, *Hum. Brain Mapp.* 14 (2001) 140–151, <http://dx.doi.org/10.1002/hbm.1048>.
 [41] E.A. Allen, E. Damaraju, S.M. Plis, E.B. Erhardt, T. Eichele, V.D. Calhoun, Tracking whole-brain connectivity dynamics in the resting state, *Cereb. Cortex* 24 (2014) 663–676, <http://dx.doi.org/10.1093/cercor/bhs352>.
 [42] J. Seubert, J. Freiherr, J. Frasnelli, T. Hummel, J.N. Lundström, Orbitofrontal cortex and olfactory bulb volume predict distinct aspects of olfactory performance in healthy subjects, *Cereb. Cortex* 23 (2013) 2448–2456, <http://dx.doi.org/10.1093/cercor/bhs230>.
 [43] G. Liakakis, J. Nickel, R.J. Seitz, Diversity of the inferior frontal gyrus—A meta-analysis of neuroimaging studies, *Behav. Brain Res.* 225 (2011) 341–347, <http://dx.doi.org/10.1016/j.bbr.2011.06.022>.
 [44] M. Vigneau, V. Beaucousin, P.Y. Hervé, H. Duffau, F. Crivello, O. Houdé, B. Mazoyer, N. Tzourio-Mazoyer, Meta-analyzing left hemisphere language areas: phonology, semantics, and sentence processing, *Neuroimage* 30 (2006) 1414–1432, <http://dx.doi.org/10.1016/j.neuroimage.2005.11.002>.
 [45] F.I.M. Craik, E. Tulving, Depth of processing and the retention of words in episodic memory, *J. Exp. Psychol. Gen.* 104 (1975) 268–294, <http://dx.doi.org/10.1037/0096-3445.104.3.268>.
 [46] F.I.M. Craik, R.S. Lockhart, Levels of processing: a framework for memory research, *J. Verbal Learning Verbal Behav.* 11 (1972) 671–684, [http://dx.doi.org/10.1016/S0022-5371\(72\)80001-X](http://dx.doi.org/10.1016/S0022-5371(72)80001-X).
 [47] J.A. Gottfried, Central mechanisms of odour object perception, *Nat. Rev. Neurosci.* 11 (2010) 628–641, <http://dx.doi.org/10.1038/nrn2883>.
 [48] D.M. Johnson, K.R. Illig, M. Behan, L.B. Haberly, New features of connectivity in piriform cortex visualized by intracellular injection of pyramidal cells suggest that primary olfactory cortex functions like association cortex in other sensory systems, *J. Neurosci.* 20 (2000) 6974–6982.
 [49] C. Zelano, M. Bensafi, J. Porter, J. Mainland, B. Johnson, E. Bremner, C. Telles, R. Khan, N. Sobel, Attentional modulation in human primary olfactory cortex, *Nat. Neurosci.* 8 (2005) 114–120, <http://dx.doi.org/10.1038/nn1368>.
 [50] M.E. Raichle, A.M. MacLeod, A.Z. Snyder, W.J. Powers, D.A. Gusnard, G.L. Shulman, A default mode of brain function, *Proc. Natl. Acad. Sci. U. S. A.* 98 (2001) 676–682.
 [51] M.E. Raichle, The brain's default mode network, *Annu. Rev. Neurosci.* 38 (2015) 433–447, <http://dx.doi.org/10.1146/annurev-neuro-071013-014030>.
 [52] K. Christoff, A.M. Gordon, J. Smallwood, R. Smith, J.W. Schooler, Experience sampling during fMRI reveals default network and executive system contributions to mind wandering, *Proc. Natl. Acad. Sci. U. S. A.* 106 (2009) 8719–8724, <http://dx.doi.org/10.1073/pnas.0900234106>.
 [53] B. Clemens, M. Zvyagintsev, A. Sack, A. Heinecke, K. Willmes, W. Sturm, Revealing the functional neuroanatomy of intrinsic alertness using fMRI: Methodological peculiarities, *PLoS One* 6 (2011) e25453, <http://dx.doi.org/10.1371/journal.pone.0025453>.
 [54] J.A. Gottfried, A.P.R. Smith, M.D. Rugg, R.J. Dolan, Remembrance of odors past: human olfactory cortex in cross-modal recognition memory, *Neuron* 42 (2004) 687–695, [http://dx.doi.org/10.1016/S0896-6273\(04\)00270-3](http://dx.doi.org/10.1016/S0896-6273(04)00270-3).
 [55] M.W. Cole, W. Schneider, The cognitive control network: integrated cortical regions with dissociable functions, *Neuroimage* 37 (2007) 343–360, <http://dx.doi.org/10.1016/j.neuroimage.2007.03.071>.
 [56] S. Zhang, C.S.R. Li, Functional networks for cognitive control in a stop signal task: independent component analysis, *Hum. Brain Mapp.* 33 (2012) 89–104, <http://dx.doi.org/10.1002/hbm.21197>.
 [57] T.A. Niendam, A.R. Laird, K.L. Ray, Y.M. Dean, D.C. Glahn, C.S. Carter, Meta-analytic evidence for a superordinate cognitive control network subserving diverse executive functions, *Cogn. Affect. Behav. Neurosci.* 12 (2012) 241–268, <http://dx.doi.org/10.3758/s13415-011-0083-5>.
 [58] C. Sestieri, M. Corbetta, G.L. Romani, G.L. Shulman, Episodic memory retrieval, parietal cortex, and the default mode network: functional and topographic analyses, *J. Neurosci.* 31 (2011) 4407–4420, <http://dx.doi.org/10.1523/JNEUROSCI.3335-10.2011>.
 [59] M. Ystad, T. Eichele, A.A.J. Lundervold, A.A.J. Lundervold, Subcortical functional connectivity and verbal episodic memory in healthy elderly—a resting state fMRI study, *Neuroimage* 52 (2010) 379–388, <http://dx.doi.org/10.1016/j.neuroimage.2010.03.062>.
 [60] S. Smith, Environmental context-dependent memory, *Mem. Context Context Mem.* 8 (2001) 13–34, <http://dx.doi.org/10.3758/BF03196157>.
 [61] U. Lueken, M. Muehlhan, R. Evens, H.U. Wittchen, C. Kirschbaum, Within and between session changes in subjective and neuroendocrine stress parameters during magnetic resonance imaging: a controlled scanner training study, *Psychoneuroendocrinology* 37 (2012) 1299–1308, <http://dx.doi.org/10.1016/j.psycheneu.2012.01.003>.
 [62] H.A. Chapman, D. Bernier, B. Rusak, MRI-related anxiety levels change within and between repeated scanning sessions, *Psychiatry Res.* 182 (2010) 160–164, <http://dx.doi.org/10.1016/j.pscychres.2010.01.005>.